Progress In Electromagnetics Research M, Vol. 62, 99–109, 2017

Transmission Line Model Considering Nonuniform Temperature Distribution at Different Locations

Yanling Wang[1, *], Yang Mo[1], Likai Liang[1], Wei Wang[2], Xiaofeng Zhou[3], and Ran Wei[4]

Abstract—The temperature variation throughout overhead transmission lines has an important effect on the line operation. In order to describe the actual operation of transmission lines more accurately, this paper proposes a line segmentation method based on temperature distribution at different locations. Taking the actual transmission line of Shaanxi Province as a test case, the influence of the different temperature calculation methods on the maximum transmission power of lines is studied under the lumped parameter model and the distributed parameter model, respectively. It is shown that the transmission line model considering nonuniform temperature distribution at different locations is more accurate for studying the operating state of the system.

1. INTRODUCTION

Long-distance transmission lines in large-scale power systems are usually equivalent to uniform distributed parameter models or lumped parameter models. The models need to meet some assumptions. For example, current density is uniform; the physical characteristics of the transmission lines remain constant; the surrounding external environment parameters are constant. These models do not take into account meteorological condition changes throughout transmission lines. The whole line uses preset seasonal meteorological conditions in [1, 2]. The whole line uses real-time meteorological parameter values in [3, 4]. They all use the uniform meteorological conditions along the line, regardless of the locations.

However, the meteorological parameters along the lines, such as ambient temperature, are nonuniform at different locations, especially in extreme weather conditions [5]. There is a certain error in the previous assumption. The change of the ambient temperature distribution along the long-distance transmission line causes the corresponding changes in the line temperature and in its impedance. Thus, the line parameters do not have uniform distribution. When the transmission distance is very long, it is necessary to consider the nonuniform distribution of impedance parameters.

By segmenting transmission lines, the specific parameters of each segment can be considered to improve the accuracy of the power grid system analysis. Three methods were offered to indicate the temperature of lines in [6]. The study shows that considering the temperature of the steel-reinforced aluminum conductor can improve the accuracy of the model prediction. When the transmission line load was short circuited or broken, the influence of transmission line segmentation model on the spectrum was analyzed in [7]. The line segmentation method was provided based on frequency and temperature in [8] and [9, 10] respectively, which were carried out in hardware experiment at power system laboratory in Drexel University. These researches focus on the influence of the frequency and

Received 12 September 2017, Accepted 24 October 2017, Scheduled 11 November 2017

* Corresponding author: Yanling Wang (wangyanling@sdu.edu.cn).

[1] School of Mechanical, Electrical and Information Engineering, Shandong University, Weihai, Shandong 264209, China. [2] School of Electrical Engineering and Automation, Shandong University of Science and Technology, Tai'an, Shandong 271019, China. [3] Department of Mechanical and Electrical Engineering, Weihai Vocational College, Weihai, Shandong 264210, China. [4] Shandong Inspur Software Company Limited, Jinan, Shandong 250014, China.

temperature segmentation on the system load flow wave attenuation and phase changes. The difference between the lumped parameter model and distributed parameter model was analyzed by simulation for long-distance transmission lines in [11].

Different from above researches, this paper studies the influence of the temperature distribution on the impedance of long-distance transmission lines. A multi-segment line model is proposed to represent the nonuniform distribution of the temperature along transmission lines. The maximum transmission powers of transmission line, under different temperature distribution models, are studied, which can provide reference for accurately assessing the system state in order to ensure the safety operation of power grids.

This paper is organized as follows. Section 2 introduces the traditional lumped parameter model, distributed parameter model and three methods dealing with the line temperature distribution. Section 3 proposes a multi-segment line model and presents a segmentation method for long-distance transmission lines. In Section 4, different transmission capabilities of different models are investigated for an actual transmission line in Shaanxi Province, China. Section 5 gives a detailed summary and further considerations of this paper.

2. TRANSMISSION LINE MODELS BASED ON TEMPERATURE DISTRIBUTION IN SPACE

2.1. Lumped Parameter Model of Transmission Line

The resistance and reactance of transmission lines are related to the conductor temperature. The unit length resistance can be defined as follows:

$$r_l = \frac{\rho}{S} \tag{1}$$

where r_l is the resistance in per unit length of the line; ρ is the resistivity; S is the rated sectional area. In the practical applications, it is generally possible to obtain a resistance value at a conductor temperature of 20°C. When the actual conductor temperature is not 20°C, the resistance value needs to be corrected as follows:

$$r_t = r_{20}[1 + \alpha(t - 20)] \tag{2}$$

where r_t is the resistance value when the conductor temperature is t°C; r_{20} is the resistance value when the conductor temperature is 20°C; α is the temperature coefficient of resistance, usually defined as 0.0039 [12].

The reactance x_l in per unit length of the three-phase transmission line is related to its geometric mean distance D_m and the radius of the transmission line r_l, as shown next line:

$$x_l = 0.1445 \lg \frac{D_m}{r_l} + 0.0157 \tag{3}$$

where $D_m = \sqrt[3]{D_{\mathrm{ab}} D_{\mathrm{bc}} D_{\mathrm{ca}}}$, and $D_{\mathrm{ab}}, D_{\mathrm{bc}}, D_{\mathrm{ca}}$ are the distances among the three pairs of lines.

For bundle conductors, the unit reactance is related to the geometric mean distance D_m of the line, the number of bundle conductor n in per phase, and the equivalent radius r_{eq}. The function is shown as follows:

$$x_l = 0.1445 \lg \frac{D_m}{r_{\mathrm{eq}}} + \frac{0.0157}{n} \tag{4}$$

where $r_{\mathrm{eq}} = \sqrt[n]{r_l(d_{12} d_{13} \ldots d_{1n})}$, and $d_{12}, d_{13}, \ldots, d_{1n}$ are the distances between this line and other lines.

Like resistance, the reactance of transmission lines varies with conductor temperature, as shown in Eq. (5):

$$x_t = x_{20}[1 + \beta(t - 20)] \tag{5}$$

where x_t is the reactance when the conductor temperature is t°C; x_{20} is the reactance when the conductor temperature is 20°C; β is the temperature coefficient of the line reactance, usually defined as 0.0039.

2.2. Distributed Parameter Model of Transmission Line

When the length of the overhead transmission line is more than 300 km, it is regarded as a long-distance transmission line. It is necessary to consider the distributed parameter characteristics when we calculate impedance and admittance. The parameters are defined as Eq. (6) and Eq. (7):

$$Z' = \sqrt{\frac{r_l + jx_l}{jb_l}} \sinh\left[\sqrt{(r_l + jx_l)jb_l} \times l\right] \tag{6}$$

$$Y' = 2\sqrt{\frac{jb_l}{r_l + jx_l}} \times \frac{\cosh\left[\sqrt{(r_l + jx_l)jb_l} \times l\right] - 1}{\sinh\left[\sqrt{(r_l + jx_l)jb_l} \times l\right]} \tag{7}$$

where Z' and Y' are the impedance and admittance, respectively, when considering distributed parameter characteristics; l is the length of the line; r_l, x_l and b_l are the resistance, reactance and susceptance in per unit length respectively.

2.3. Three Methods of Calculating Transmission Line Temperature

2.3.1. Seasonal Temperature

For the parameters of transmission lines, the conductor temperature of the whole transmission line is represented by the preset temperature according to different seasons.

2.3.2. Average Temperature

We suppose that the temperature varies linearly along the transmission line. The beginning temperature of the transmission line is T_{beg}, and the end temperature of the transmission line is T_{end}. Then the average temperature T_{avg} of the beginning and the end is defined as follows:

$$T_{\text{avg}} = \frac{T_{\text{beg}} + T_{\text{end}}}{2} \tag{8}$$

2.3.3. Weighted Average Temperature

We suppose that the number of temperature known points along the transmission line is N_t, and the temperature of each temperature known point is T_i, $i = 1, 2, \ldots, N_t$. $\Delta x_{i,i+1}$, $i = 1, 2, \ldots, N_t - 1$ is the distance between point i and point $i + 1$. Then the weighted average temperature T_{wavg} is defined as:

$$T_{\text{wavg}} = \sum_{i=1}^{N_t - 1} \left[\left(\frac{T_i + T_{i+1}}{2}\right) \times \frac{\Delta x_{i,i+1}}{l}\right] \tag{9}$$

When there are only two temperature known points in the line, which are the beginning and end points, the weighted average temperature is the average temperature of the beginning and the end. Thus the average temperature of the beginning and the end is a particular case of the weighted average temperature [13].

3. SEGMENTATION METHOD OF LONG-DISTANCE TRANSMISSION LINES

For a long-distance transmission line, the conductor temperature will change along the line, and it will cause changes in the line impedance. The segmentation of transmission lines is a good method to consider the nonuniform temperature distribution. This paper studies the segmentation method under the condition that certain temperature points are known, in order to accurately calculate the impedance value of each segment. There are three steps for the segmentation method of long-distance transmission lines in the following section.

3.1. Determination of the Temperature at the Beginning and End of the Segmented Line

In order to describe the temperature distribution trend along the transmission line, we need to determine the temperature known points of the line. We assume that the first and last temperature known points are outside the beginning and end of the segmented line, as shown in Fig. 1.

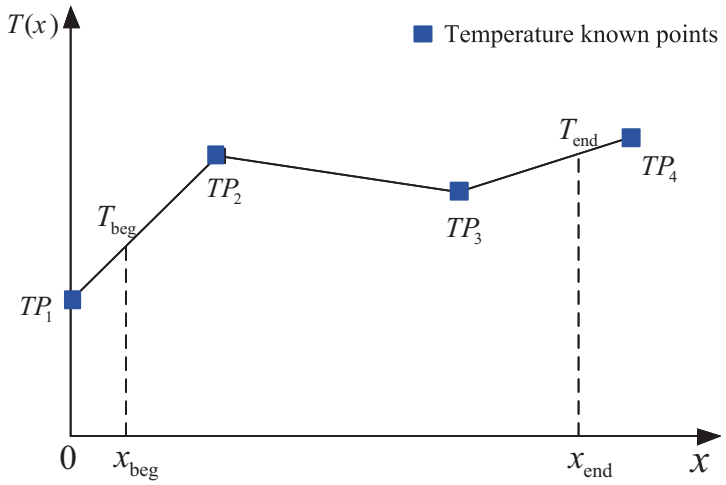

Figure 1. The temperature distribution trend along the line.

In Fig. 1, TP_i $(i = 1, 2, 3, 4)$ are temperature known points, which means the points where the temperature is known. x is the distance from $x = 0$. $T(x)$ is the temperature at the location of x. x_{beg} and x_{end} are the beginning and end points of the line. T_{beg} and T_{end} are the temperatures of the beginning and end points, respectively. Assuming that the line temperature between temperature known points varies linearly along the distance, T_{beg} and T_{end} can be easily obtained.

3.2. Determination of the Check Points of the Segmented Line

After determining temperatures at the beginning and end of the long-distance line, we need to determine the check points. Suppose that the line is divided into N parts on average. N can be calculated by Eq. (10):

$$N = \lceil l / \min(x_{\text{AB}}, x_{\text{begC}}, x_{\text{endD}}) \rceil \tag{10}$$

where x_{AB} is the distance of any temperature known points A and B. x_{begC} is the distance between the beginning point and adjacent point C. x_{endD} is the distance between the end point and adjacent point D. $\lceil\rceil$ means positive rounding. After determining N, we get the distance between the adjacent check points by $\Delta x = l/N$. The locations of check points are defined by $\mu \times \Delta x$ $(\forall \mu = 0, 1, \ldots, N)$. When $\mu = 0$, the check point is the beginning point x_{beg}. When $\mu = N$, the check point is the end point x_{end}, as shown in Fig. 2.

3.3. Segmentation of the Long-Distance Transmission Line

We assume that N_{seg} is the number of segments of the transmission line. $i(1 \le i \le N)$ and $j(2 \le j \le N + 1)$ are the check points, and their corresponding temperature are T_i and T_j. We need to set temperature threshold ΔT before segmentation. If the temperature difference of different checkpoints and temperature threshold meet Eq. (11), it indicates that the line between check points needs to be segmented.

$$\begin{aligned} &\text{if} \quad \left\lceil \frac{|T_i - T_j|}{\Delta T} \right\rceil \ge 1 \\ &\text{then} \quad N_{\text{seg}} = N_{\text{seg}} + 1 \end{aligned} \tag{11}$$

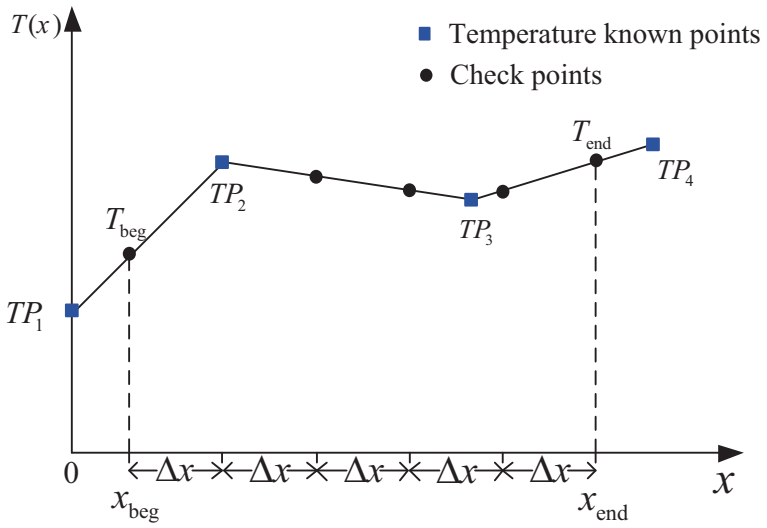

Figure 2. Determination of the check points.

After the segmentation, the number of segments and corresponding positions are obtained. The average temperature of the check points i, j at each end of the segment is the temperature of the segment, as shown in Eq. (12).

$$T_{\text{seg}_{ij}} = (T_i + T_j)/2 \tag{12}$$

The corresponding impedance value of each segment can be obtained by the temperature, and the influence of the segment on the line power transmission can be analyzed.

4. CASE STUDY

This section takes the 750 kV transmission line from Yuheng to Xinyi of Shaanxi Province as an example, whose type is bundle conductor. The phase spacing is 17.4 m, and the bundle spacing is 0.4 m. When the temperature is 20°C, the resistance in per unit length is 0.0131 Ω/km, and the reactance in per unit length is 0.2704 Ω/km. Susceptance in per unit length is 4.0910×10^{-6}S/km, and the length of the line is 386.7 km.

We study the power voltage curve of its lumped parameter model and distributed parameter model in different temperature calculation methods. In the stable region which is made of steady state solution of power flow calculation, as the load increases, the operating point gradually turns to the boundary of the static voltage stability region. In the border running state, as the load continues to increase, a voltage instability will occur. The corresponding state before the voltage instability is called the critical state of voltage stability. At this point, the system has the maximum power transmission capacity. In addition, ambient conditions such as humidity and insolation are assumed constant in this section. The conductor temperature of the transmission line is assumed to be consistent with the ambient temperature, and we just use the "temperature" below. The temperature is derived from the data in Table 1.

4.1. Segmentation of the Long-Distance Transmission Line

In this case, the beginning point x_{beg} is Yuheng, and the end point x_{end} is Xinyi. The sequence number of the temperature known points and the detailed data are shown in Table 1, and "distance" is the distance between current position and Yuheng in this table.

From Table 1, we can get $\min(x_{\text{AB}}, x_{\text{begA}}, x_{\text{endA}}) = 17.3$ km. According to Eq. (10), we can get $N = 23$, and the distance between the adjacent check points of the line is 16.8130 km. The distribution of temperature known points and check points in the line are shown in Fig. 3.

Table 1. Data of the temperature known points along transmission lines.

Serial number	Longitude (E)	Latitude (N)	Temperature (°C)	Distance (km)
1	109.676	37.989	22.31258	0
2	109.844	37.095	23.60006	102.1
3	109.792	36.671	22.68975	148.4
4	109.695	36.243	23.97541	197.1
5	109.404	35.666	21.78378	266.7
6	109.515	35.166	23.27094	323.0
7	109.688	34.771	18.89304	369.4
8	109.823	34.685	19.47246	386.7

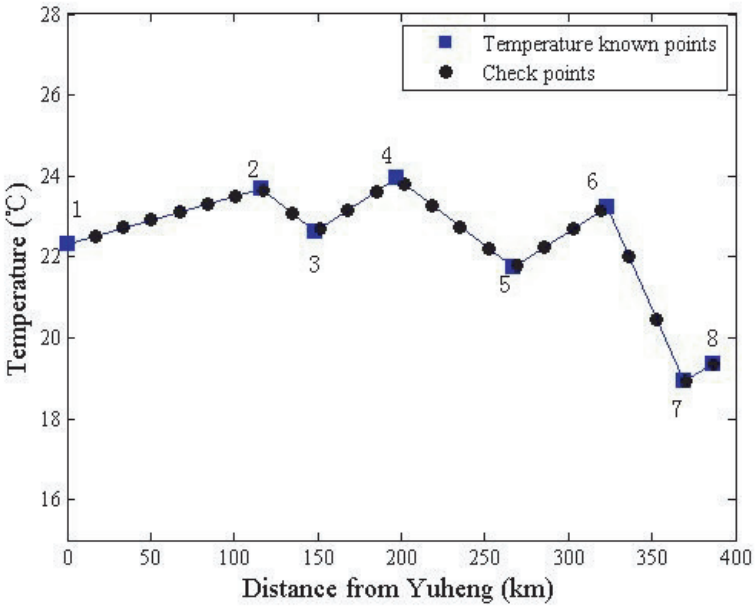

Figure 3. The temperature known points and check points in the line.

After determining the check points, we achieve the segmentation method by a MATLAB program written according to the segmentation process shown in Section 3. The temperature threshold ΔT is set as 3.5°C. The line is divided into five segments, and segmentation results are shown in Table 2.

Table 2. Segmented parameters when ΔT is 3.5°C.

Segment number	Length of segment (km)	Temperature (°C)	Resistance (Ω/km)	Reactance (Ω/km)
1	201.7565	23.0681	0.013257	0.27364
2	67.2522	22.7998	0.013243	0.27335
3	50.4391	22.4669	0.013226	0.27300
4	33.6261	21.7942	0.013192	0.27229
5	33.6261	19.8939	0.013095	0.27029

4.2. The Power Voltage Curves of the Lumped Parameter Model

In different situations of segmentation, seasonal temperature, average temperature and weighted average temperature, the power of load is gradually increased from 5 MW to the maximum acceptable load of the system. In this paper, seasonal temperature T_{seas} is selected as 17°C. T_{avg} and T_{wavg} are 20.8925°C and 22.5456°C, respectively, which are drawn from Eq. (8) and Eq. (9).

According to Eq. (2) and Eq. (3), the line parameters corresponding to the seasonal temperature T_{seas}, average temperature T_{avg} and weighted average temperature of T_{wavg} are shown in Table 3.

Table 3. Line parameters at different temperatures in the lumped parameter model.

Parameters	T_{seas}	T_{avg}	T_{wavg}
Resistance (Ω/km)	0.01295	0.01314	0.01323
Reactance (Ω/km)	0.26736	0.27128	0.27308

According to the parameters in Table 3, the PV curves and maximum acceptable load by means of system equivalence and simplication are shown in Fig. 4. Without considering the distributed parameter characteristics, the maximum power $P_{\max}$ and its corresponding voltage V_{load} of the critical states in different situations are shown in Table 4.

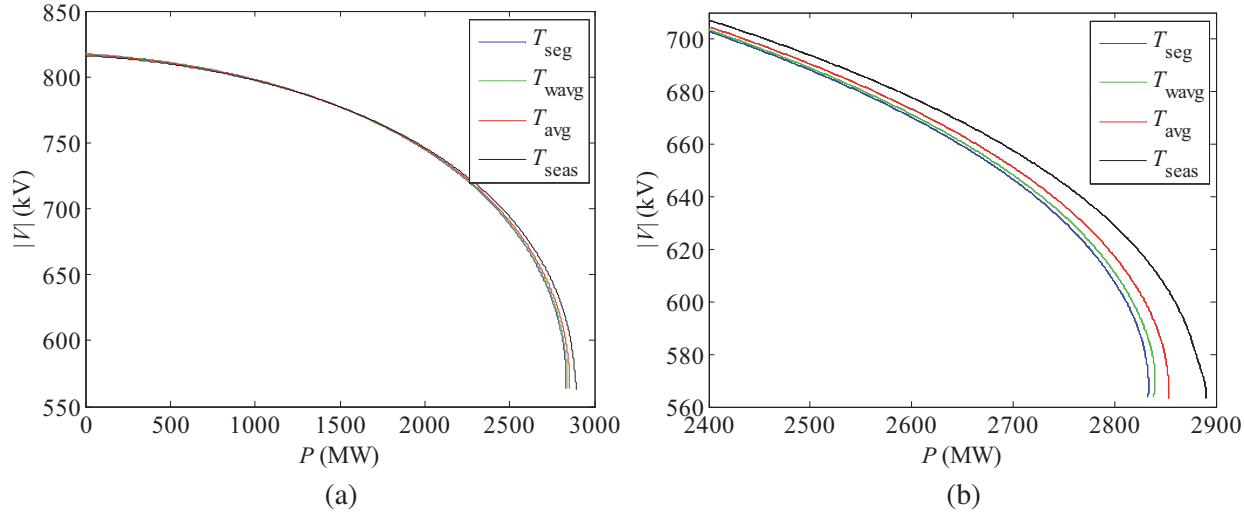

Figure 4. PV curves of the lumped parameter model: (a) PV curves, (b) zoomed in around the critical state.

Table 4. Parameters of critical state of system in the lumped parameter model.

Critical state	T_{seg}	T_{wavg}	T_{avg}	T_{seas}
$P_{\max}$ (MW)	2832.98	2838.50	2853.49	2890.79
V_{load} (kV)	563.64	563.64	563.43	562.67

From Fig. 4 and Table 4, the corresponding system critical states are different when the transmission lines are at different temperatures. The difference of V_{load} is not obvious, but the difference of $P_{\max}$ is obvious. The maximum power of T_{seas} is 2.04% higher than the maximum power of T_{seg}. The maximum power of T_{wavg} is 0.195% higher than the maximum power of T_{seg}. It means that the result of the weighted temperature method is closer to that of the segment method.

4.3. The Power Voltage Curves of the Distributed Parameter Model

Because the line is a long-distance transmission line, the distributed parameter characteristics should be considered. According to Eq. (6) and Eq. (7), considering the distributed parameter characteristics, the impedances related to seasonal temperature T_{seas}, average temperature T_{avg} and weighted average temperature T_{wavg} are shown in Table 5.

Table 5. Line parameters at different temperatures in the distributed parameter model.

Parameters	T_{seas}	T_{avg}	T_{wavg}
Resistance (Ω/km)	0.01278	0.01269	0.01251
Reactance (Ω/km)	0.26839	0.26665	0.26286

According to the parameters in Table 5, the PV curves and maximum acceptable load are shown in Fig. 5. When considering the distributed parameter characteristics, the maximum power $P_{\max}$ and its corresponding voltage V_{load} of the critical states in different situations are shown in Table 6.

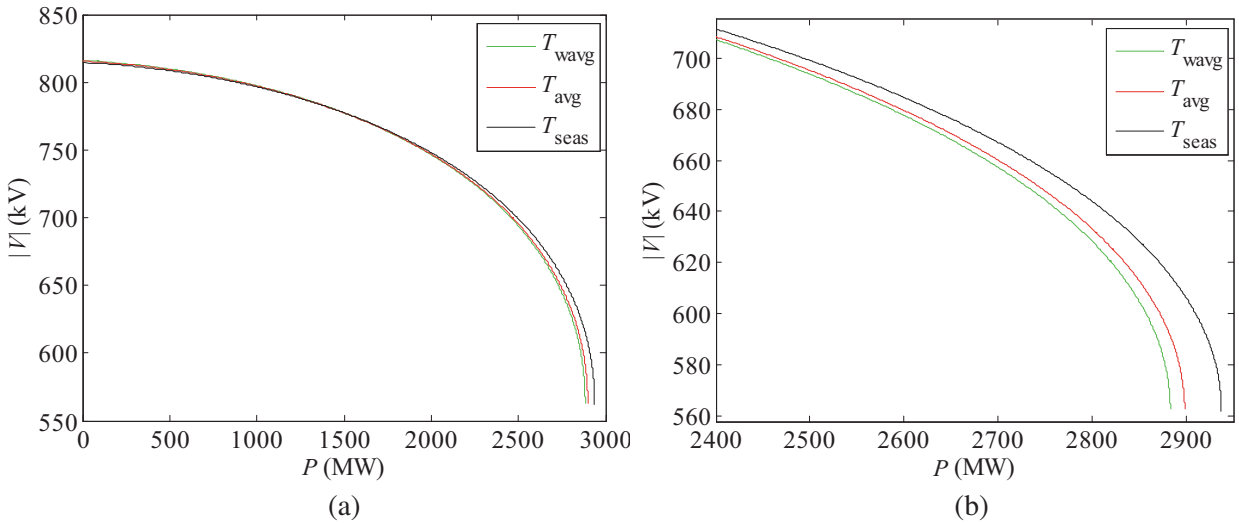

Figure 5. PV curves of the distributed parameter model: (a) PV curves, (b) zoomed in around the critical state.

Table 6. Parameters of critical state of system in the distributed parameter model.

Critical state	T_{wavg}	T_{avg}	T_{seas}
$P_{\max}$ (MW)	2882.99	2898.29	2937.09
V_{load} (kV)	563.09	562.72	562.13

As can be seen from Table 6, when the temperature is low, the power $P_{\max}$ is high. The $P_{\max}$ of T_{seas} is 1.88% higher than the $P_{\max}$ of T_{wavg}. The $P_{\max}$ of T_{avg} is 0.53% higher than the $P_{\max}$ of T_{wavg}. When the system reaches the critical state, the lower the temperature is, the lower impedance value of the line is, and the greater the maximum of the transmission power is. Thus, maximum transmission power is affected by the temperature distribution of the line in the power system. In addition, compared to Table 4 and Table 6, the maximum transmission power of the distributed parameter model is different from the lumped parameter model under the same temperature. The maximum difference value is 1.66% in the case of T_{seas}. Therefore, it is necessary to use the distributed parameter model for long-distance

transmission lines. However, the distributed parameter model, compared to the multi-segment model, still cannot account for the non-uniform distribution of temperature along the line.

4.4. The Influence of the Temperature Threshold on the PV Curves

In this section, we study the effect of the different temperature thresholds on the segmentation results of the line. When ΔT is 1.5°C, the studied line is divided into 14 segments. When ΔT is 6°C, the studied line is divided into 3 segments. The segmentation results are shown in Table 7 and Table 8, and the corresponding power voltage curves are shown in Fig. 6.

Table 7. Segmentation result when $\Delta T = 1.5$°C.

Serial number	Length of segment (km)	Temperature (°C)	Resistance (Ω/km)	Reactance (Ω/km)
1	16.8130	22.4257	0.013224	0.27296
2	50.4391	22.8166	0.013244	0.27337
3	50.4391	23.3722	0.013272	0.27396
4	33.6261	23.1707	0.013262	0.27374
5	33.6161	23.1660	0.013262	0.27374
6	16.8130	23.7168	0.013289	0.27432
7	33.6261	23.2701	0.013267	0.27385
8	33.6261	22.2617	0.013216	0.27279
9	33.6261	22.2417	0.013215	0.27276
10	16.8130	22.9172	0.013249	0.27348
11	16.8130	22.5745	0.013315	0.27311
12	16.8130	21.2264	0.013163	0.27169
13	16.8130	19.6910	0.013084	0.27007
14	16.8130	19.1410	0.013056	0.26949

Table 8. Segmentation result when $\Delta T = 6$°C.

Serial number	Length of segment (km)	Temperature (°C)	Resistance (Ω/km)	Reactance (Ω/km)
1	201.7563	23.0681	0.013257	0.27364
2	151.3171	22.1272	0.013209	0.27264
3	33.6262	19.8931	0.013095	0.27029

Table 9. Parameters of critical state of system.

Critical state	$\Delta T = 1.5$°C	$\Delta T = 3.5$°C	$\Delta T = 6$°C
$P_{\max}$ (MW)	2829.61	2832.98	2841.09
V_{load} (kV)	563.38	563.64	563.63

The maximum power $P_{\max}$ and its corresponding voltage V_{load} of the critical state in different situations are shown in Table 9.

It can be seen from Table 9 that the $P_{\max}$ of $\Delta T = 1.5$°C is 0.12% lower than $\Delta T = 3.5$°C and 0.41% lower than $\Delta T = 6$°C. The smaller the threshold is, the more complex the calculation is, but the

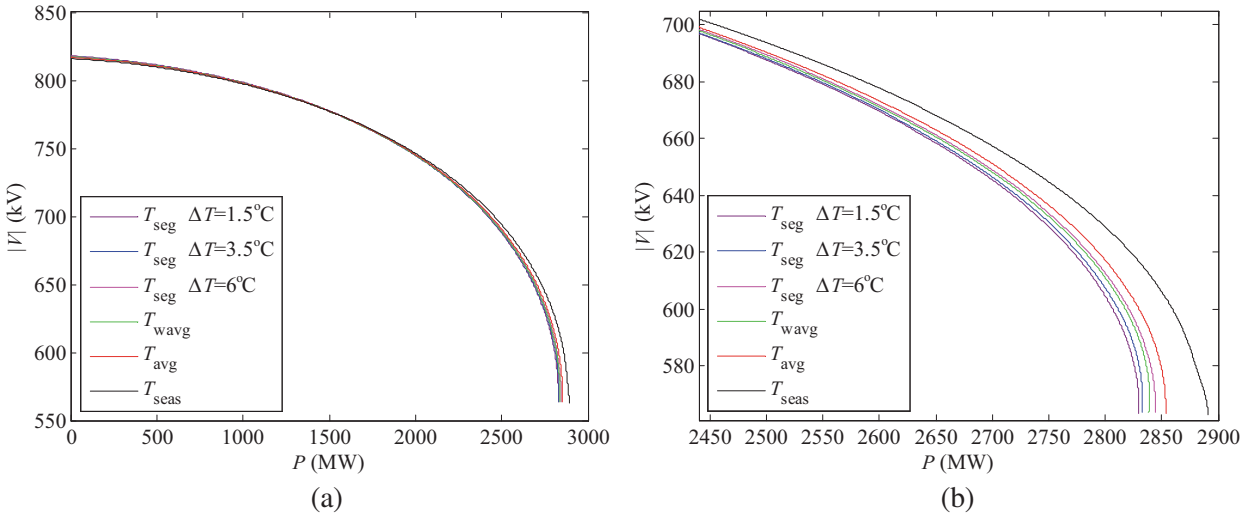

Figure 6. PV curves of different temperature thresholds: (a) PV curves, (b) zoomed in around the critical state.

more appropriate the calculation results are to the actual system. In addition, as shown in Fig. 6, when the temperature threshold is large, the corresponding PV curve of T_{seg} is closer to the PV curve of T_{avg}. Combining Table 7 and Table 8, the larger the value of ΔT is, the smaller the number of segments is. When ΔT is pretty large ($\Delta T \geq 10°\text{C}$ in this case), the line is reduced to one segment, and the PV curve coincides with the curve of T_{avg}. Considering the temperature distribution along the line and segmenting it are beneficial to getting more accurate maximum transmission power and voltage, which will more accurately assess the power transmission capacity of the power system.

5. CONCLUSIONS

This paper studies the influence of temperature on the transmission line. We propose a long-distance transmission line segmentation method. The main steps of segmentation method are given. We study the effect of temperature on maximum power and its corresponding voltage under different methods, such as seasonal temperature, average temperature, weighted average temperature, and segmentation temperature. We can conclude that for the first three temperature calculated methods, considering the distributed characteristics of the line, the calculation results will be more accurate. The fourth method is an accurate method to consider the nonuniform distribution of the line temperature at different locations. In order to obtain the accurate maximum acceptable load of the system, it is necessary to consider the temperature nonuniform distribution and use the segmentation method on the transmission line. In the future, other environmental parameter distributions will be considered along transmission lines, such as wind speed.

ACKNOWLEDGMENT

This paper is supported by the National Natural Science Foundation of China (51407111, 51407106, 51641702), the Science & Technology Development Project of Shandong Province (ZR2015ZX045), and the Science and Technology Development Project of Weihai City (2014DXGJ23).

REFERENCES

1. Heckenbergerova, J., P. Musilek, and K. Filimonenkov, "Assessment of seasonal static thermal ratings of overhead transmission conductors," *IEEE Power and Energy Society General Meeting*, 1–8, 2011.

2. Beers, G. M., S. R. Gilligan, H. W. Lis, and J. M. Schamberger, "Transmission conductor ratings," *IEEE Transactions on Power Apparatus and Systems*, Vol. 82, No. 68, 767–775, 1963.
3. Fu, J., D. J. Morrow, S. Abdelkader, and B. Fox, "Impact of dynamic line rating on power systems," *46th International Universities' Power Engineering Conference*, 1–5, 2011.
4. Greenwood, D. M. and P. C. Taylor, "Investigating the impact of real-time thermal ratings on power network reliability," *IEEE Transactions on Power Systems*, Vol. 29, No. 5, 2460–2468, 2014.
5. Barry, R. G. and R. J. Chorley, *Atmosphere, Weather and Climate*, 8th Edition, Routledge, New York, 2003.
6. Wydra, M. and P. Kacejko, "Power system state estimation using wire temperature measurements for model accuracy enhancement," *IEEE PES Innovative Smart Grid Technologies Conference Europe*, 1–6, 2016.
7. Wilson, G. L. and K. A. Schmidt, "Transmission line models for switching studies: Design criteria II. Selection of section length, model design and tests," *IEEE Transaction on Power Apparatus and Systems*, Vol. 93, No. 1, 389–395, 1974.
8. Cecchi, V., A. S. Leger, K. Miu, and C. O. Nwankpa, "Modeling approach for transmission lines in the presence of non-fundamental frequencies," *IEEE Transaction on Power Delivery*, Vol. 24, No. 4, 2328–2335, 2009.
9. Cecchi, V., A. S. Leger, K. Miu, and C. O. Nwankpa, "Incorporating temperature variations into transmission-line models," *IEEE Transactions on Power Delivery*, Vol. 26, No. 4, 2189–2196, 2011.
10. Rahman, M., M. Kiesau, and V. Cecchi, "Investigating the impacts of conductor temperature on power handling capabilities of transmission lines using a multi-segment line model," *SoutheastCon 2017*, 1–7, 2017.
11. Tang, Y., H. Chen, H. Wang, F. Dai, and S. Jiang, "Transmission line models used in travelling wave studies," *Transmission and Distribution Conference*, 797–803, 1999.
12. Bockarjova, M. and G. Andersson, "Transmission line conductor temperature impact on state estimation accuracy," *IEEE Lausanne Power Tech.*, 701–706, 2007.
13. Wydra, M. and P. Kacejko, "Power system state estimation accuracy enhancement using temperature measurements of overhead line conductors," *PES Innovative Smart Grid Technologies Conference Europe*, 183–192, 2016.